Criticality Benchmark Results

Using Various MCNP Data Libraries

Los Alamos
N A T I O N A L   L A B O R A T O R Y

Edited by Sheila Molony, Group CIC-1

An Affirmative Action/Equal Opportunity Employer

*Criticality Benchmark Results
Using Various MCNP Data Libraries*

Stephanie C. Frankle

Los Alamos
NATIONAL LABORATORY

Table of Contents

Criticality Benchmark Results Using Various MCNP Data Libraries

By

Stephanie C. Frankle

ABSTRACT

A suite of 86 criticality benchmarks has been recently implemented in MCNP™ as part of the nuclear data validation effort. These benchmarks have been run using two sets of MCNP continuous-energy neutron data: ENDF/B-VI based data through Release 2 (ENDF60) and the ENDF/B-V based data. New evaluations were completed for ENDF/B-VI for a number of the important nuclides such as the isotopes of H, Be, C, N, O, Fe, Ni, ^{235,238}U, ^{237}Np, and ^{239,240}Pu.

When examining the results of these calculations for the five major categories of ^{233}U, intermediate-enriched ^{235}U (IEU), highly enriched ^{235}U (HEU), ^{239}Pu, and mixed metal assembles, we find the following:

- The new evaluations for ^{9}Be, ^{12}C, and ^{14}N show no net effect on k_{eff}.
- There is a consistent decrease in k_{eff} for all of the solution assemblies for ENDF/B-VI due to ^{1}H and ^{16}O, moving k_{eff} further from the benchmark value for uranium solutions and closer to the benchmark value for plutonium solutions.
- k_{eff} decreased for the ENDF/B-VI Fe isotopic data, moving the calculated k_{eff} further from the benchmark value.
- k_{eff} decreased for the ENDF/B-VI Ni isotopic data, moving the calculated k_{eff} closer to the benchmark value.
- The W data remained unchanged and tended to calculate slightly higher than the benchmark values.
- For metal uranium systems, the ENDF/B-VI data for ^{235}U tends to decrease k_{eff} while the ^{238}U data tends to increase k_{eff}. The net result depends on the energy spectrum and material specifications for the particular assembly.
- For more intermediate-energy systems, the changes in the ^{235,238}U evaluations tend to increase k_{eff}. For the mixed graphite and normal uranium-reflected assembly, a large increase in k_{eff} due to changes in the ^{238}U evaluation moved the calculated k_{eff} much closer to the benchmark value.
- There is little change in k_{eff} for the uranium solutions due to the new ^{235,238}U evaluations.
- There is little change in k_{eff} for the ^{239}Pu metal assemblies, but a decrease in k_{eff} for the solution assemblies, moving them closer to the benchmark value.

MCNP is a trademark of the Regents of the University of California, Los Alamos National Laboratory.

I.   Introduction

As part of the validation process for nuclear data provided to transport codes such as MCNP,[1] we have developed a comprehensive suite of 86 criticality benchmarks.[2] In choosing these benchmarks, we tried to assemble a set of problems that would (1) test different energy regions, such as the high-energy region of the fast critical assemblies and the thermal region of the solution experiments; (2) test a variety of important reflector materials; and (3) not have an unreasonably high number of benchmarks. This benchmark suite by no means covers all isotopes and energy regions of interest. For example, we are awaiting new experimental measurements for intermediate-energy region (0.0001–0.100 MeV) critical assemblies[3] and adequate benchmark specifications for low-enrichment uranium metal assemblies. Suitable experiments utilizing ^{232}Th are also lacking.

Two compendiums of criticality experimental information were used in developing this suite of benchmarks: the Cross Section Evaluation Working Group (CSEWG) specifications[4] and the International Criticality Safety Benchmark Evaluation Project (ICSBEP).[5] The suite is composed of five major categories: critical assemblies utilizing ^{233}U, intermediate-enriched ^{235}U (IEU), highly enriched ^{235}U (HEU), ^{239}Pu, and mixed metal assemblies. Within each category, there are bare, reflected, and solution assemblies. A variety of reflector materials have been utilized, such as Be, BeO, C, Al, Fe, Ni, W, Th, ^{233}U, and normal (natural) uranium U(N). Tables 1-13 contain a brief description of each of the criticality benchmarks, including its associated MCNP filename. The notation of HEU (93.5) indicates that highly enriched uranium having 93.5 weight percent of ^{235}U was used in the experiment.

We present the list of benchmarks in a different format than that used previously in LA-13594. The benchmarks have now been placed into 13 groups: bare metal assemblies, solution experiments, water-reflected metal assemblies, assemblies reflected by polyethylene, beryllium and beryllium oxide, graphite, aluminum, steel and nickel, tungsten, thorium, normal uranium, and HEU, and other experiments.

As you will note, there are two sets of specifications for five of the assemblies. For Flattop-23, a sphere of ^{233}U reflected by normal uranium, the CSEWG specification contains a small gap between the main fuel and the reflector, whereas the ICSBEP

specification has no gap. ICSBEP specifications for Godiva contain both the standard sphere of HEU as well as nested spherical shells of HEU. There are two specifications for the one- and two-dimensional models for Bigten, and for the water-reflected sphere of HEU. The thorium-reflected sphere of ^{239}Pu, Thor, also has a one- and two-dimensional representation. Therefore, there are a total of 91 MCNP input files.

For this report, we will focus only on the results from the k_{eff} calculations. We calculated these benchmarks using two sets of MCNP continuous-energy data libraries: ENDF/B-VI based data through Release 2 (ENDF60)[6] and the ENDF/B-V based data. Table 14 lists the ZAIDs used. A future report will detail the specifications for other measured quantities such as neutron leakage spectra, activation ratio measurements with a variety of materials, and central-fission ratio measurements for nine of the critical assemblies.[7] Additionally, we will include fission-ratio measurements performed at NIST (National Institute of Standards and Technology). A brief description of the nuclear data libraries used in the calculations is given in the next section, followed by a discussion of the k_{eff} results. The results of sensitivity tests performed to determine which nuclide was driving the changes in k_{eff} between data libraries are also presented.

Table 1: Criticality Benchmark Descriptions for Bare Metal Assemblies

MCNP Filename	1D/2D/3D	Benchmark Description
23umt1	1D	Jezebel-23, Bare Sphere of U-233
ieumt3	1D	Bare IEU Sphere (36 wt.%), VNIIEF
umet1ss	1D	Godiva, Unreflected Sphere of HEU, Simple Sphere representation
umet1ns	1D	Godiva, Unreflected Sphere of HEU, Nested Spherical Shell representation
umet8	3D	Bare HEU Sphere, VNIITF, 3D model
umet15	2D	Bare HEU Cylinder, VNIITF
umet18	1D	Simplified Bare HEU Sphere, VNIIEF
pumet1	1D	Jezebel-Pu (4.5%), Bare Sphere of Pu-239 with 4.5% Pu-240
pumet2	1D	Jezebel-Pu (20%), Bare Sphere of Pu-239 with 20% Pu-240
pumet22	1D	Simplified Plutonium (98%) Bare Sphere, VNIIEF

Table 2: Criticality Benchmark Descriptions for Solution Assemblies

MCNP Filename	1D/2D/3D	Benchmark Description
23usl1a	1D	ORNL-5, 1.0226 g/l Unreflected 27.24" Sphere of U-233 nitrate solution
23usl1b	1D	ORNL-6, 1.0253 g/l Unreflected 27.24" Sphere of U-233 nitrate solution with Boron
23usl1c	1D	ORNL-7, 1.0274 g/l Unreflected 27.24" Sphere of U-233 nitrate solution with Boron
23usl1d	1D	ORNL-8, 1.0275 g/l Unreflected 27.24" Sphere of U-233 nitrate solution with Boron
23usl1e	1D	ORNL-9, 1.0286 g/l Unreflected 27.24" Sphere of U-233 nitrate solution with Boron
23usl8	1D	ORNL-11, 1.0153 g/l Unreflected 48.04" Sphere of U-233 nitrate solution with Boron
usol13a	1D	ORNL-1, Unreflected Sphere of Uranyl (20.12 g/l) Nitrate
usol13b	1D	ORNL-2, Unreflected Sphere of Uranyl (23.53 g/l) Nitrate with Boron
usol13c	1D	ORNL-3, Unreflected Sphere of Uranyl (26.77 g/l) Nitrate with Boron
usol13d	1D	ORNL-4, Unreflected Sphere of Uranyl (28.45 g/l) Nitrate with Boron
usol32	1D	ORNL-10, Unreflected Sphere of Uranyl (28.45 g/l) Nitrate with Boron
pnl1	1D	PNL-1, Idealized (No Container) Unreflected Sphere of Pu Nitrate Solution
pnl6	1D	PNL-6, Idealized (No Container) Unreflected Sphere of Pu Nitrate Solution; Revised PNL-2
pusl11a	1D	PNL-3, Unreflected 18" Sphere of Pu (22.35 g/l) Nitrate Solution
pusl11b	1D	PNL-4, Unreflected 18" Sphere of Pu (27.49 g/l) Nitrate Solution
pusl11c	1D	PNL-5, Unreflected 16" Sphere of Pu (43.43 g/l) Nitrate Solution
pusl11d	1D	Unreflected 16" Sphere of Pu (34.96 g/l) Nitrate Solution

**Table 3: Criticality Benchmark Descriptions for
Water-Reflected Metal Assemblies**

MCNP Filename	1D/2D/3D	Benchmark Description
umet4a	2D	Water-Reflected HEU (97.675) Sphere, with Plexiglas ring
umet4b	2D	Water-Reflected HEU (97.675) Sphere, *Trans. Am. Nuc. Soc.* **27**, pg. 412 (1977)
pumet11	1D	Water-Reflected alpha-phase Pu sphere

**Table 4: Criticality Benchmark Descriptions for
Polyethylene-Reflected Assemblies**

MCNP Filename	1D/2D/3D	Benchmark Description
umet11	3D	Polyethylene (CH2)-Reflected HEU(~89.6) Sphere, VNIITF
umet20	1D	Polyethylene-Reflected HEU Sphere, VNIIEF
pumet24	1D	Simplified Plutonium Sphere, Polyethylene Reflector, VNIIEF

**Table 5: Criticality Benchmark Descriptions for
Beryllium and Beryllium Oxide-Reflected Assemblies**

MCNP Filename	1D/2D/3D	Benchmark Description
23umt5a	1D	0.805" Be-Reflected Sphere of U-233, Planet Assembly
23umt5b	1D	1.652" Be-Reflected Sphere of U-233, Planet Assembly
umet9a	3D	Be-Reflected HEU (~89.6) Sphere, VNIITF
umet9b	3D	BeO-Reflected HEU (~89.6) Sphere, VNIITF
pumet18	1D	Be-Reflected Pu (94.79) Sphere, Planet Assembly
pumet19	3D	Be-Reflected Pu (~90) Sphere, VNIITF
pumt21a	2D	Be-Reflected Pu Cylinder
pumt21b	2D	BeO-Reflected Pu Cylinder

Table 6: Criticality Benchmark Descriptions for Graphite-Reflected Assemblies

MCNP Filename	1D/2D/3D	Benchmark Description
ieumt4	1D	Graphite-Reflected IEU Sphere (36 wt.%), VNIIEF
umet19	1D	Graphite-Reflected HEU Sphere, VNIIEF
pumet23	1D	Simplified Plutonium Sphere, Graphite reflector, VNIIEF

Table 7: Criticality Benchmark Descriptions for Aluminum-Reflected Assemblies

MCNP Filename	1D/2D/3D	Benchmark Description
ieumt6	1D	Duralumin-Reflected IEU Sphere (36 wt.%), VNIIEF
umet12	3D	Aluminum-Reflected HEU (~89.6) Sphere, VNIITF
umet22	1D	Duralumin-Reflected HEU Sphere, VNIIEF
pumet9	1D	Aluminum-Reflected Pu (94.8) Sphere, Comet Assembly

Table 8: Criticality Benchmark Descriptions for Steel- and Nickel-Reflected Assemblies

MCNP Filename	1D/2D/3D	Benchmark Description
		Fe-Reflected
ieumt5	1D	Steel-Reflected IEU Sphere (36 wt.%), VNIIEF
umet13	3D	St.20 Steel-Reflected HEU (~89.6) Sphere, VNIITF
umet21	1D	Steel-Reflected HEU Sphere, VNIIEF
pumet25	1D	Simplified Plutonium Sphere, 1.55-cm Steel Reflector, VNIIEF
pumet26	1D	Simplified Plutonium Sphere, 11.9-cm Steel Reflector, VNIIEF
		Ni-Reflected
umet3l	1D	8.0" Nickel-Reflected HEU (93.5) Sphere, Topsy Assembly

Table 9: Criticality Benchmark Descriptions for
Tungsten-Reflected Assemblies

MCNP Filename	1D/2D/3D	Benchmark Description
23umt4a	1D	0.96" Tungsten-Reflected Sphere of U-233, Planet Assembly
23umt4b	1D	2.28" Tungsten-Reflected Sphere of U-233, Planet Assembly
umet3h	1D	1.9" Tungsten Carbide-Reflected HEU (93.5) Sphere, Topsy Assembly
umet3i	1D	2.9" Tungsten Carbide-Reflected HEU (93.5) Sphere, Topsy Assembly
umet3j	1D	4.5" Tungsten Carbide-Reflected HEU (93.5) Sphere, Topsy Assembly
umet3k	1D	6.5" Tungsten Carbide-Reflected HEU (93.5) Sphere, Topsy Assembly
pumet5	1D	Tungsten-Reflected Pu (94.79) Sphere, Planet Assembly

Table 10: Criticality Benchmark Descriptions for
Thorium-Reflected Assemblies

MCNP Filename	1D/2D/3D	Benchmark Description
pumet8a	1D	Thorium-Reflected Pu (93.59) Sphere, Thor Assembly, 1D Model
pumet8b	2D	Thorium-Reflected Pu (93.59) Sphere, Thor Assembly, 2D Model

Table 11: Criticality Benchmark Descriptions for
Normal Uranium-Reflected Assemblies

MCNP Filename	1D/2D/3D	Benchmark Description
23umt3a	1D	0.906" Normal Uranium-Reflected Sphere of U-233, Planet Assembly
23umt3b	1D	2.09" Normal Uranium-Reflected Sphere of U-233, Planet Assembly
23umt6	1D	Flattop-23, 7.84" Normal Uranium-Reflected Sphere of U-233
flat23	1D	Flattop-23, CSEWG, U(N)-Reflected U-233 Sphere + Gap
ieumt2	2D	Reflected Jemima, U(N)-Reflected Cylindrical Disks of HEU and Natural Uranium
umet3a	1D	2" Tuballoy-Reflected HEU (93.5) Sphere, Topsy Assembly
umet3b	1D	3" Tuballoy-Reflected HEU (93.5) Sphere, Topsy Assembly
umet3c	1D	4" Tuballoy-Reflected HEU (93.5) Sphere, Topsy Assembly
umet3d	1D	5" Tuballoy-Reflected HEU (93.5) Sphere, Topsy Assembly
umet3e	1D	7" Tuballoy-Reflected HEU (93.5) Sphere, Topsy Assembly
umet3f	1D	8" Tuballoy-Reflected HEU (93.5) Sphere, Topsy Assembly
umet3g	1D	11" Tuballoy-Reflected HEU (93.5) Sphere, Topsy Assembly
umet14	3D	Depleted Uranium-Reflected HEU (~89.6) Sphere, VNIITF
umet28	1D	Flattop-25, U(N)-Reflected HEU Sphere
bigten1	1D	Bigten, 1D Model: U(N)-Reflected Uranium Sphere
bigten2	2D	Bigten, 2D Model: U(N)-Reflected Uranium Cylinder
pumet6	1D	Normal Uranium-Reflected Pu (93.80) Sphere, Flattop Assembly
pumet10	1D	U(N)-Reflected Pu Sphere
pumet20	3D	Depleted Uranium-Reflected Pu (~90) Sphere, VNIITF

**Table 12: Criticality Benchmark Descriptions for
Highly Enriched Uranium-Reflected Assemblies**

MCNP Filename	1D/2D/3D	Benchmark Description
23umt2a	1D	0.481" HEU-Reflected Sphere of U-233; Planet Assembly
23umt2b	1D	0.783" HEU-Reflected Sphere of U-233, Planet Assembly
mixmet1	1D	HEU-Reflected Pu Sphere, Planet Assembly
mixmet3	3D	HEU-Reflected Pu Sphere, VNIITF

Table 13: Criticality Benchmark Descriptions for Other Assemblies

MCNP Filename	1D/2D/3D	Benchmark Description
ieumt1a	2D	Jemima 1, Cylindrical Disks of HEU and Natural Uranium
ieumt1b	2D	Jemima 2, Cylindrical Disks of HEU and Natural Uranium
ieumt1c	2D	Jemima 3, Cylindrical Disks of HEU and Natural Uranium
ieumt1d	2D	Jemima 4, Cylindrical Disks of HEU and Natural Uranium
mixmet8	3D	ZEBRA 8A/2, Graphite and Natural Uranium-Reflected Pu

II.   Nuclear Data Libraries

The benchmark suite was run using MCNP version 4B with two sets of nuclear data: ENDF/B-VI based data through Release 2 and ENDF/B-V based data (see Table 14). The ENDF/B-VI Release 2 data are contained in the ENDF60 nuclear data library. The ENDF/B-V based data are contained in a number of data libraries (RMCCS, ENDF5P, ENDF5U, etc.) and are composed of data having a ZAID ending of ".50c" or ".55c". The ".50c" indicates that the data were from ENDF/B-V Release 0. In particular, ".55c" data were used for the following nuclides: ^{2}H, ^{11}B, Fe, ^{182,183,184,186}W, ^{237}Np, and ^{239}Pu. The replacement ZAID, 40000.56c, for the original ".50c" data file was used for Zr.

Most of the important evaluations used in these benchmarks had major changes from B-V to B-VI. Evaluations which remained essentially unchanged are ^{27}Al, Ga, ^{182,183,184,186}W, ^{232}Th, ^{233,234}U, and ^{242}Pu. The ".55c" tungsten data were accepted for ENDF/B-V Release 2, and hence are equivalent to the ".60c" in ENDF60. Photon production data were added to the ^{233}U evaluation in 1981, but this update will have no effect on k$_{eff}$ calculations. The only differences between data sets for the unchanged evaluations are from changes in the processing of the evaluation into an MCNP data file

using NJOY[8] and *should* not be significant. Some of the major nuclides of interest were completely reevaluated for ENDF/B-VI. These include evaluations for the naturally occurring isotopes of Cr, Fe, Ni, and Cu. In the actinide region, ^{235,238}U and ^{239,241}Pu were completely updated, including an extension of the resonance region much higher in energy. These evaluation changes have been described elsewhere in more detail.[9] For each benchmark, we used isotopic evaluations instead of elemental evaluations whenever possible, such as for the W isotopes.

Table 14: ZAIDS Used from the Two Libraries

Element	ENDF/B-V	ENDF/B-VI	Element	ENDF/B-V	ENDF/B-VI
H	1001.50c	1001.60c	Ni	28000.50c	28058.60c
	1002.55c	1002.60c			28060.60c
Be	4009.50c	4009.60c			28061.60c
	5010.50c	5010.60c			28062.60c
	5011.55c	5011.60c			28064.60c
C	6000.50c	6000.60c	Cu	29000.50c	29063.60c
N	7014.50c	7014.60c			29065.60c
O	8016.50c	8016.60c	Ga	31000.50c	31000.60c
Na	11023.50c	11023.60c	Zr	40000.56c	40000.60c
Mg	12000.50c	12000.60c	Mo	42000.50c	42000.60c
Al	13027.50c	13027.60c	Cd	48000.50c	48000.60c
Si	14000.50c	14000.60c	W	74182.55c	74182.60c
P	15031.50c	15031.60c		74183.55c	74183.60c
S	16032.50c	16032.60c		74184.55c	74184.60c
Ca	20000.50c	20000.60c		74186.55c	74186.60c
Ti	22000.50c	22000.60c	Th	90232.50c	90232.60c
V	23000.50c	23000.60c	U	92233.50c	92233.60c
Cr	24000.50c	24050.60c		92234.50c	92234.60c
		24052.60c		92235.50c	92235.60c
		24053.60c		92236.50c	92236.60c
		24054.60c		92238.50c	92238.60c
Mn	25055.50c	25055.60c	Np	93237.55c	93237.60c
Fe	26000.55c	26054.60c	Pu	94239.55c	94239.60c
		26056.60c		94240.50c	94240.60c
		26057.60c		94241.50c	94241.60c
		26058.60c		94242.50c	94242.60c
			Am	95241.50c	95241.60c

III. k_{eff} Results

Most of the calculations were performed on an HP-735 workstation. The solution assemblies and sensitivity calculations were performed on the Blue Mountain cluster of SGI Origin 2000s. There are a number of different ways to view the k_{eff} results for these benchmarks. We have chosen to present the results by reflector material, or lack thereof. We have also grouped all of the solution assemblies together. When examining the results of the calculations by the five major categories of [233]U, intermediate-enriched [235]U (IEU), highly enriched [235]U (HEU), [239]Pu, and mixed metal assemblies, we find that on average there are few major changes in the results for the nonsolution [233]U, IEU, [239]Pu, and mixed metal assemblies. We do see a small decrease in k_{eff} on average for the HEU metal assemblies (-0.0011±0.0002) from the ENDF/B-V to the ENDF/B-VI Release 2 libraries. There is a consistent decrease in k_{eff} for all of the solution assemblies between the B-V and B-VI libraries.

We will now examine the 13 sets of benchmarks in more detail. All results are quoted at the 2σ level, which represents a confidence level of 95% that the true k_{eff} for the calculation lies within the value quoted +/- 2σ. When one is considering this many benchmark calculations (~100), we can expect to see a few true k_{eff} values that will lie outside of the quoted range based on statistics.

A.   Bare Metal Assemblies

There are 9 bare metal assemblies in this suite of benchmarks. The Godiva assembly has two geometry descriptions: a simple sphere (umet1ss) and nested spherical shells (umet1ns) of HEU. Table 15 details the results for the bare metal assemblies and gives the benchmark k_{eff} value. From these results we can see that the small changes in processing for the [233]U data make little difference in the calculated k_{eff} value, and that the calculated k_{eff} value is low. The one intermediate-enriched uranium benchmark (ieumt3, having 36 wt.% [235]U and 63 wt.% [238]U) shows a significant decrease between the B-V and B-VI data libraries, due to the changes in the [235]U evaluation. As we will see later in Section III.K for the normal uranium-reflected assemblies, the changes to the [235]U evaluation tend to decrease k_{eff}, while the changes to the [238]U evaluation tend to increase k_{eff}. For any given assembly, the energy spectrum and ratio

of ^{235}U to ^{238}U will determine the net effect. The highly enriched uranium benchmarks tend to show a slight decrease in the k_{eff} value, while the ^{239}Pu benchmarks show little change.

Table 15: Criticality Benchmark Results for Bare Metal Assemblies

| MCNP Filename	Benchmark k_{eff}	ENDF/B-V	ENDF60
23umt1	1.000±0.001	0.9942±0.0011	0.9931±0.0011
ieumt3	1.0000±0.0017	1.0051±0.0012	1.0005±0.0012
umet1ss	1.000±0.001	0.9982±0.0011	0.9963±0.0012
umet1ns	1.000±0.001	0.9975±0.0012	0.9968±0.0011
umet8	0.9989±0016	0.9942±0.0012	0.9918±0.0011
umet15	0.9996±0.0017	0.9931±0.0011	0.9925±0.0011
umet18	1.0000±0.0016	0.9984±0.0011	0.9969±0.0012
pumet1	1.000±0.002	0.9969±0.0012	0.9971±0.0010
pumet2	1.000±0.002	0.9979±0.0011	0.9992±0.0011
pumet22	1.0000±0.0021	0.9965±0.0011	0.9962±0.0011

B.   Solution Assemblies

Table 16 presents the results for the solution assemblies. With no exception, there is a significant decrease in k_{eff} from B-V to B-VI data libraries. For the ^{233}U and ^{235}U solutions, the decrease tends to move the calculations away from the benchmark value. The results for the ^{239}Pu solutions, however, are moved toward the benchmark value for k_{eff}. We performed a large number of sensitivity tests for these assemblies. In each case, we used ENDF/B-V data for all isotopes, except the isotope of interest, where we used ENDF60 data. We then computed the mean value for the change in k_{eff} for the set of assemblies. On average, the new ^{1}H evaluation decreased k_{eff} by 0.0010±0.0001, while ^{16}O decreased k_{eff} by 0.0026±0.0002. There was no net effect due to the new ^{14}N evaluation. The ^{239}Pu evaluation tended to decrease k_{eff} by 0.0033±0.0004 for the plutonium solutions, and changes in the ^{235}U evaluation made very little difference in uranium solutions.

12

Table 16: Criticality Benchmark Results for Solution Assemblies

MCNP Filename	Benchmark k_{eff}	ENDF/B-V	ENDF60
23usl1a	1.0000±0.0031	1.0010±0.0007	0.9967±0.0008
23usl1b	1.0005±0.0033	1.0004±0.0008	0.9966±0.0008
23usl1c	1.0006±0.0033	0.9997±0.0008	0.9969±0.0008
23usl1d	0.9998±0.0033	0.9993±0.0008	0.9962±0.0008
23usl1e	0.9999±0.0033	0.9984±0.0008	0.9956±0.0007
23usl8	1.0006±0.0029	0.9987±0.0005	0.9954±0.0005
usol13a	1.0012±0.0026	1.0007±0.0008	0.9972±0.0007
usol13b	1.0007±0.0036	0.9993±0.0008	0.9964±0.0008
usol13c	1.0009±0.0036	0.9952±0.0009	0.9922±0.0008
usol13d	1.0003±0.0036	0.9981±0.0009	0.9957±0.0009
usol32	1.0015±0.0026	1.0003±0.0005	0.9966±0.0005
pnl1	1.0 (a)	1.0158±0.0013	1.0062±0.0012
pnl6	1.0 (a)	1.0089±0.0013	1.0020±0.0013
pusl11a	1.0000±0.0052	1.0019±0.0011	0.9951±0.0011
pusl11b	1.0000±0.0052	1.0084±0.0012	0.9998±0.0011
pusl11c	1.0000±0.0052	1.0137±0.0013	1.0045±0.0012
pusl11d	1.0000±0.0052	1.0182±0.0012	1.0085±0.0012

(a) Specific benchmark values were not given in the CSEWG specifications, and are assumed to be 1.0.
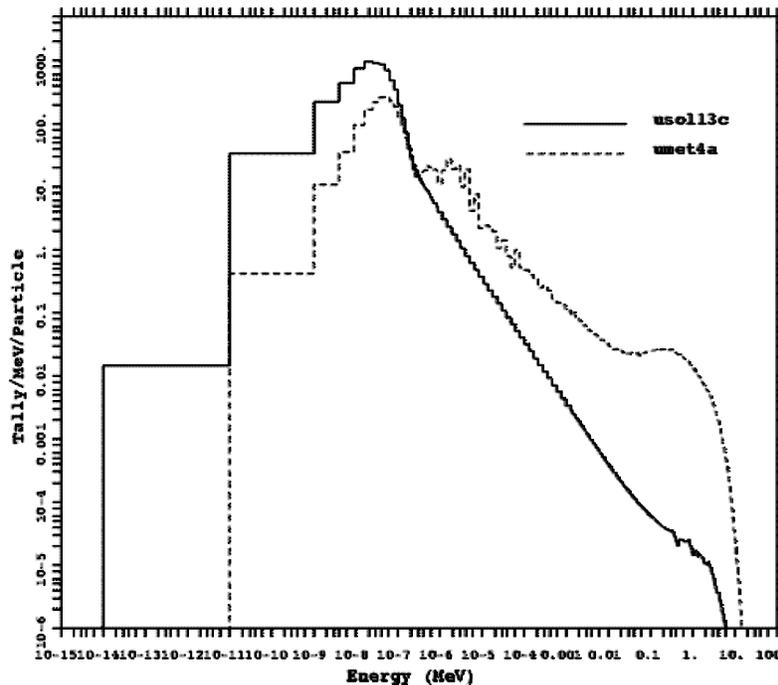
Figure 1: Comparison of Neutron Flux Spectra for USOL13C and UMET4A.

C. Water-Reflected Metal Assemblies

There are 2 water-reflected assemblies. The water-reflected HEU sphere also has two descriptions: umet4a is a more complicated geometry, having the Plexiglas support ring included, and umet4b is a simpler geometry of the HEU sphere in a cylindrical tank of water.

Table 17 displays the results for the water-reflected spheres. There is an increase in k_{eff} for the water-reflected HEU sphere, which is a net result of the new evaluation for hydrogen and oxygen that lowered k_{eff} and the [235]U evaluation that increased k_{eff}. Recall that there was little change in k_{eff} due to the [235]U evaluation for the solution assemblies (Section III.B). The water-reflected HEU sphere (umet4a) has a harder neutron energy spectrum and a greater mass of [235]U than the uranium solution assemblies do. Hence, different energy regions of the evaluation are being exercised to differing extents. To illustrate this point, Figure 1 shows a comparison of the neutron energy spectrum over the solution assembly for usol13c with the central HEU sphere for umet4a.

The opposite trends due to changes in the [235]U evaluation for the metal systems in Section III.A and the water-reflected sphere of HEU can be understood by comparing the neutron energy spectrum over the core region of ieumt3 with umet4a. As Figure 2 shows, the neutron energy spectrum of umet4a is more of an intermediate energy spectrum and is softer than that of ieumt3.

**Table 17: Criticality Benchmark Results for
Water-Reflected Metal Assemblies**

MCNP Filename	Benchmark k_{eff}	ENDF/B-V	ENDF60
umet4a	1.002	0.9999±0.0014	1.0010±0.0015
umet4b	1.0003±0.0005	0.9967±0.0015	0.9969±0.0015
pumet11	1.0000±0.001	1.0009±0.0014	0.9984±0.0014
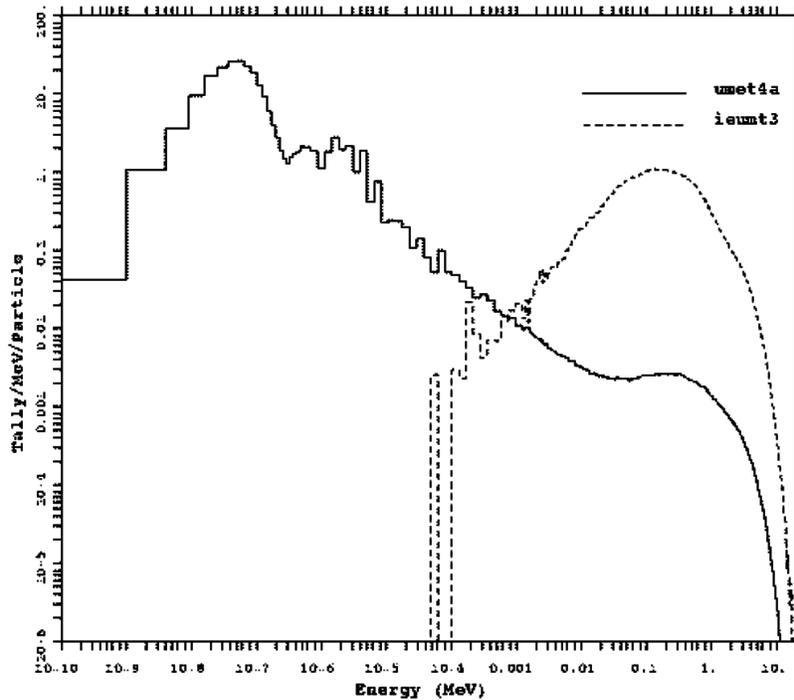
Figure 2: Comparison of Neutron Flux Spectrum for UMET4A and IEUMT3.

D. Polyethylene-Reflected Assemblies

Table 18 presents the calculational results for the polyethylene (CH_2)-reflected assemblies. The solution experiments discussed previously in Section III.B indicated that there was a small decrease in k_{eff} due to changes in the hydrogen evaluation. We performed sensitivity studies using B-V data for all isotopes except carbon, where we used ENDF60 data. These studies showed that changes to the carbon evaluation had a relatively negligible effect on k_{eff} for these benchmarks.

Table18: Criticality Benchmark Results for
Polyethylene-Reflected Assemblies

MCNP Filename	Benchmark k_{eff}	ENDF/B-V	ENDF60
umet11	1.000±0.001	0.9924±0.0014	0.9954±0.0014
umet20	1.0000±0.0030	0.9958±0.0013	0.9972±0.0013
pumet24	1.0000±0.0020	0.9981±0.0013	1.0009±0.0012

E.   Beryllium- and Beryllium Oxide-Reflected Assemblies

Table 19 gives the calculational results for the beryllium- and beryllium oxide-reflected assemblies. There are two benchmarks—23umt5a and umet9a—that showed a change of ~2σ for the beryllium-reflected assemblies. We ran these benchmarks again using a different starting random number (the eighth entry on the DBCN card). The new B-V and ENDF60 results for 23umt5a were 0.9940±0.0012 and 0.9941±0.0012 respectively, illustrating that this 2σ difference was due to statistical fluctuations. Sensitivity studies show that changes in the new beryllium ENDF/B-VI evaluation do not significantly affect the calculations, while the new ^{16}O evaluation lowers k_{eff} by 0.0039+/-0.0006 for the two beryllium-oxide benchmarks, umet9b and pumt21b.

Table 19: Criticality Benchmark Results for
Beryllium and Beryllium-Oxide-Reflected Assemblies

MCNP Filename	Benchmark k_{eff}	ENDF/B-V	ENDF60
23umt5a	1.0000±0.0030	0.9940±0.0012	0.9962±0.0012
23umt5b	1.0000±0.0030	0.9955±0.0013	0.9967±0.0014
umet9a	0.9992±0.0015	0.9927±0.0012	0.9958±0.0012
umet9b	0.9992±0.0015	0.9962±0.0012	0.9936±0.0012
pumet18	1.0000±0.0030	0.9999±0.0013	0.9999±0.0012
pumet19	0.9992±0.0015	1.0016±0.0013	1.0032±0.0012
pumt21a	1.0000±0.0026	1.0033±0.0013	1.0042±0.0013
pumt21b	1.0000±0.0026	0.9970±0.0012	0.9945±0.0012

F. Graphite-Reflected Assemblies

Table 20 gives the results from the calculations for the graphite-reflected assemblies. Only one assembly—ieumt4—shows a change greater than 2σ. We have seen a similar decrease in k_{eff} for all of the IEU assemblies due to the changes in the ^{235}U evaluation (-0.0042±0.0003). The ^{238}U evaluation has no significant impact on k_{eff} for the IEU assemblies. The changes to the carbon evaluation have a minimal effect on these benchmarks.

**Table 20: Criticality Benchmark Results for
Graphite-Reflected Assemblies**

MCNP Filename	Benchmark k_{eff}	ENDF/B-V	ENDF60
ieumt4	1.0000±0.0030	1.0091±0.0012	1.0051±0.0012
umet19	1.0000±0.0030	1.0040±0.0012	1.0031±0.0012
pumet23	1.0000±0.0020	0.9973±0.0012	0.9973±0.0012

G. Aluminum-Reflected Assemblies

Table 21 shows the calculational results for the aluminum-reflected assemblies. There was no change in the aluminum evaluation between B-V and B-VI data. The changes in k_{eff} from B-V to B-VI data are therefore due to changes in the fissionable isotopes. The largest change in k_{eff} is for ieumt6, which shows a decrease similar to that seen for the other IEU assemblies from ^{235}U (Section III.A, F, M).

**Table 21: Criticality Benchmark Results for
Aluminum-Reflected Assemblies**

MCNP Filename	Benchmark k_{eff}	ENDF/B-V	ENDF60
ieumt6	1.0000±0.0023	0.9964±0.0012	0.9917±0.0012
umet12	0.9992±0.0018	0.9932±0.0011	0.9941±0.0012
umet22	1.0000±0.0021	0.9919±0.0012	0.9924±0.0012
pumet9	1.0000±0.0027	1.0003±0.0012	1.0022±0.0011

H. Steel- and Nickel-Reflected Assemblies

Table 22 presents the calculational results for the steel- and nickel-reflected assemblies. New isotopic evaluations for ENDF/B-VI for the isotopes of Cr, Fe, Ni, and Cu replaced the previous elemental evaluations. The steel-reflected assemblies show a consistent decrease in k_{eff} from B-V to B-VI data. Sensitivity studies showed that there was an average decrease in k_{eff} due to the change from B-V elemental evaluation to the isotopic B-VI evaluations for iron of 0.0048±0.0006 for these benchmarks. With the exception of ieumt5, this decrease tends to move the calculated k_{eff} value further from the benchmark value. For ieumt5, the net decrease due to the changes in the Fe and ^{235}U evaluations make the calculation much closer to the benchmark.

For the nickel-reflected assembly, umet3l, sensitivity studies indicated that the change from the B-V elemental evaluation to the isotopic B-VI evaluations decreased k_{eff} by 0.0104±0.0014, moving it closer to the benchmark value.

Table 22: Criticality Benchmark Results for Steel- and Nickel-Reflected Assemblies

MCNP Filename	Benchmark k_{eff}	ENDF/B-V	ENDF60
Fe-Reflected			
ieumt5	1.0000±0.0021	1.0112±0.0011	1.0007±0.0012
umet13	0.9990±0.0015	0.9982±0.0012	0.9941±0.0013
umet21	1.0000±0.0026	1.0023±0.0012	0.9947±0.0012
pumet25	1.0000±0.0020	0.9984±0.0012	0.9963±0.0012
pumet26	1.0000±0.0024	1.0016±0.0012	0.9971±0.0012
Ni-Reflected			
umet3l	1.0000±0.0030	1.0148±0.0013	1.0049±0.0012

I. Tungsten-Reflected Assemblies

Table 23 presents the results for the tungsten-reflected assemblies. There are essentially no changes in the evaluations for tungsten isotopes between the B-V (".55c") and the B-VI data. Hence we do not expect to see large differences in the calculated k_{eff} value. Only umet3h shows a significant change in k_{eff}. We ran the ENDF60 version of this benchmark using a different random number for the starting history. The result was a k_{eff} of 1.0049±0.0006, indicating that the drop in k_{eff} was a statistical fluctuation.

**Table 23: Criticality Benchmark Results for
Tungsten-Reflected Assemblies**

MCNP Filename	Benchmark k_{eff}	ENDF/B-V	ENDF60
23umt4a	1.0000±0.0007	1.0037±0.0012	1.0031±0.0012
23umt4b	1.0000±0.0008	1.0059±0.0013	1.0049±0.0012
umet3h	1.0000±0.0050	1.0055±0.0013	1.0065±0.0013
umet3i	1.0000±0.0050	1.0053±0.0012	1.0066±0.0013
umet3j	1.0000±0.0050	1.0056±0.0012	1.0068±0.0013
umet3k	1.0000±0.0050	1.0089±0.0012	1.0094±0.0014
pumet5	1.0000±0.0013	1.0080±0.0013	1.0102±0.0012

J. Thorium-Reflected Assemblies

There are two representations, one- and two-dimensional, of the Thor assembly, as Table 24 shows. As there were no changes in the evaluation for ^{232}Th, the changes in k_{eff} for this benchmark are due to changes in the ^{239}Pu evaluation. The slight increase in k_{eff} follows the same pattern that we have seen for the Jezebel-Pu assemblies (pumet1 and pumet2) described in Section III.A.

**Table 24: Criticality Benchmark Results for
Thorium-Reflected Assemblies**

MCNP Filename	Benchmark k_{eff}	ENDF/B-V	ENDF60
pumet8a	1.0000±0.0030	1.0042±0.0012	1.0064±0.0012
pumet8b	1.000±0.0006	1.0045±0.0013	1.0072±0.0012

K. Normal Uranium-Reflected Assemblies

Table 25 gives the results for the normal uranium-reflected assemblies. There are 18 assemblies, one of which has two representations (Flattop-23). The ICSBEP geometry (23umt6) does not include a gap between the core and reflector as does the CSEWG specification (flat23). Half of the assemblies show a change in the calculated k_{eff} of more than 2σ. The results are somewhat difficult to interpret as changes in both the ^{235}U and ^{238}U evaluations have competing effects. On average for these assemblies,

the change in the ^{235}U evaluation caused a decrease in k_{eff} of 0.0022±0.0002, while the changes in the ^{238}U evaluation caused an increase in k_{eff} of 0.0012±0.0002. For assemblies having small net changes in k_{eff}, the competing effects of the changes in the uranium evaluations tended to cancel each other. For example, in Bigten the changes to the ^{235}U evaluation decreased k_{eff} by 0.0065, while the changes to the ^{238}U evaluation increased k_{eff} by 0.0084.

Table 25: Criticality Benchmark Results for
Normal Uranium-Reflected Assemblies

MCNP Filename	Benchmark k_{eff}	ENDF/B-V	ENDF60
23umt3a	1.0000±0.0010	0.9974±0.0011	0.9971±0.0011
23umt3b	1.0000±0.0010	0.9983±0.0012	0.9991±0.0012
23umt6	1.0000±0.0014	0.9992±0.0013	0.9997±0.0014
flat23	1.000±0.001	1.0030±0.0013	1.0034±0.0013
ieumt2	1.000±0.003	1.0081±0.0011	1.0034±0.0011
umet3a	1.0000±0.0050	0.9954±0.0012	0.9920±0.0012
umet3b	1.0000±0.0050	0.9956±0.0012	0.9936±0.0012
umet3c	1.0000±0.0050	1.0006±0.0013	0.9979±0.0013
umet3d	1.0000±0.0030	0.9984±0.0012	0.9950±0.0012
umet3e	1.0000±0.0030	1.0029±0.0012	1.0014±0.0013
umet3f	1.0000±0.0030	1.0018±0.0012	1.0006±0.0013
umet3g	1.0000±0.0030	1.0039±0.0013	1.0019±0.0013
umet14	0.9989±0.0017	0.9972±0.0013	0.9957±0.0012
umet28	1.0000±0.0030	1.0030±0.0012	1.0027±0.0013
bigten1	0.996±0.003	1.0059±0.0010	1.0069±0.0010
bigten2	0.996±0.003	1.0035±0.0009	1.0045±0.0009
pumet6	1.0000±0.0030	1.0039±0.0013	1.0040±0.0014
pumet10	1.0000±0.0018	0.9984±0.0012	1.0005±0.0012
pumet20	0.9993±0.0017	0.9998±0.0012	0.9997±0.0013

L.   Highly Enriched Uranium-Reflected Assemblies

Table 26 gives the results for the highly enriched uranium-reflected assemblies. The first two benchmarks, 23umt2a and 23umt2b, have a ^{233}U core, while mixmet1 and mixmet3 have a ^{239}Pu core. Recall that the evaluation for ^{233}U did not change from B-V to B-VI (Section II). The decrease in k_{eff} for 23umt2b illustrates that the larger the HEU

reflector, the larger the decrease in k_{eff}. We see a similar trend for the two benchmarks having a [239]Pu core.

**Table 26: Criticality Benchmark Results for
Highly Enriched Uranium-Reflected Assemblies**

MCNP Filename	Benchmark k_{eff}	ENDF/B-V	ENDF60
23umt2a	1.0000±0.0010	0.9952±0.0011	0.9961±0.0011
23umt2b	1.0000±0.0011	0.9991±0.0011	0.9968±0.0011
mixmet1	1.0000±0.0016	0.9966±0.0012	0.9969±0.0012
mixmet3	0.9993±0.0016	1.0000±0.0012	0.9979±0.0012

M. Other Assemblies

Table 27 presents the results for other assemblies. The ieumt1 (Jemima) series of benchmarks are cylindrical disks of HEU and normal uranium. The MCNP model is slightly idealized, but still maintains the heterogeneous description of the disks. It has been shown that performing a criticality calculation using a homogenous material gives too large a discrepancy in k_{eff}.[5] The changes to the [235]U evaluation tend to decrease k_{eff} for the Jemima assemblies (-0.0032±0.0004), and are greater than changes in k_{eff} due the new [238]U evaluation. As discussed previously in Section III.F, this same trend is evident in all of the IEU assemblies.

Table 27: Criticality Benchmark Results for Other Assemblies

MCNP Filename	Benchmark k_{eff}	ENDF/B-V	ENDF60
mixmet8	0.9920±0.0063	0.9591±0.0009	0.9918±0.0010
ieumt1a	0.9989	1.0024±0.0012	0.9961±0.0012
ieumt1b	0.9997	1.0018±0.0012	0.9974±0.0012
ieumt1c	0.9993	1.0035±0.0012	0.9988±0.0012
ieumt1d	1.0002	1.0039±0.0012	0.9984±0.0012

The mixmet8 assembly is a rectangular graphite- and normal uranium-reflected slab of [239]Pu illustrated in Figure 3. This is a k_∞ calculation such that the geometry in

Figure 3 has periodic boundaries for the outer surfaces normal to the x- and z-axes shown in the figure. The outer surfaces perpendicular to the y-axis are reflective. For more details on the geometry, see the MIX-MET-FAST-008 specifications in reference 5.

There is a large discrepancy in the mixmet8 calculations using ENDF/B-V to B-VI data. This change in k_{eff} is due to changes in the evaluation for ^{238}U. Sensitivity tests showed that there was little effect from the new evaluations for ^{235}U, ^{239}Pu, and ^{54,56,57,58}Fe, but that the ^{238}U evaluation increased k_{eff} by 0.0265±0.0007. Figures 4–6 illustrate the difference in neutron flux through the Pu, graphite (C), and U regions for the B-V and B-VI calculations. These figures show a systematic increase in the neutron flux below 10 keV for the ENDF/B-VI data. This result is most probably due to changes in the ^{238}U evaluation below 10 keV, where the resonance region was reevaluated and extended from 4 keV to 10 keV for ENDF/B-VI. Figure 7 illustrates how thermal the neutron energy spectrum is for mixmet8 when compared to other uranium-reflected benchmarks such as Bigten. Therefore, the resonance region has a greater impact on k_{eff}. Figures 8 and 9 illustrate the changes in the total cross section and total nubar data for ^{238}U in the lower energy regions. These changes substantially improve the ^{238}U evaluation for use in thermal systems.
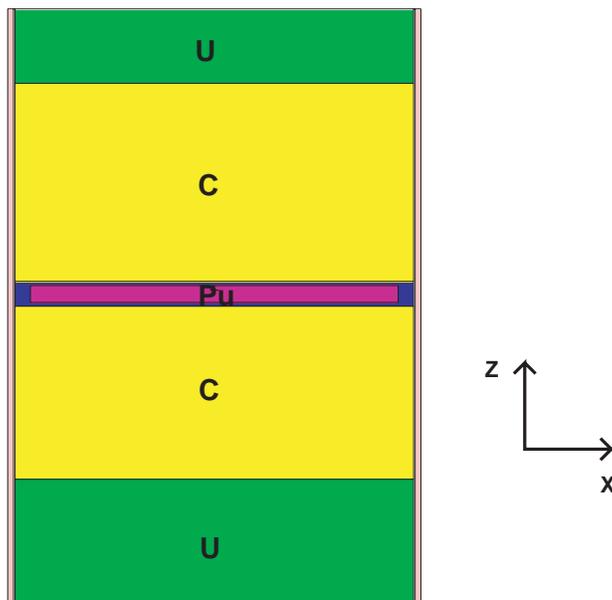
Figure 3: The Graphite and Normal Uranium-Reflected Slab of ^{239}Pu Geometry, MIXMET8. The outer surfaces are periodic.

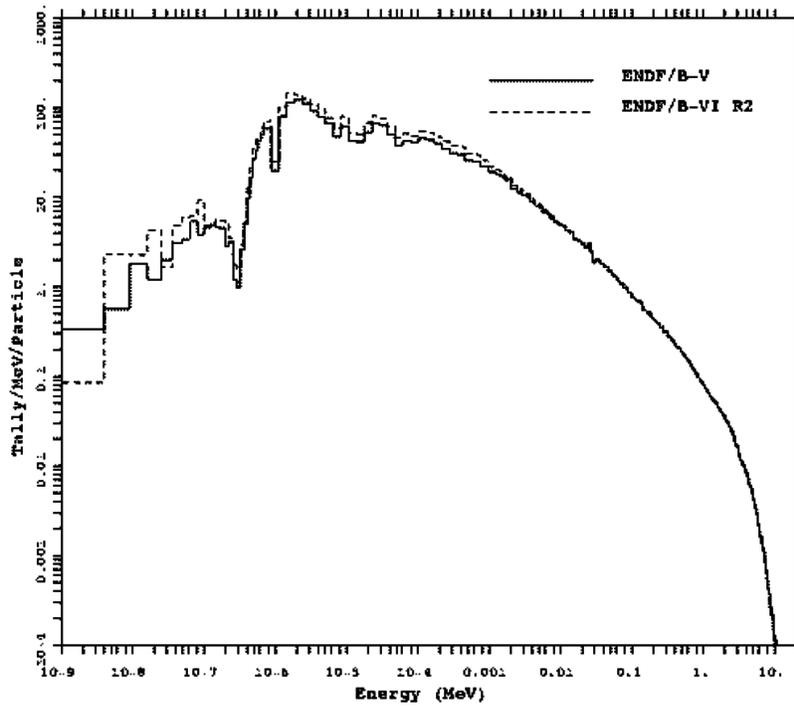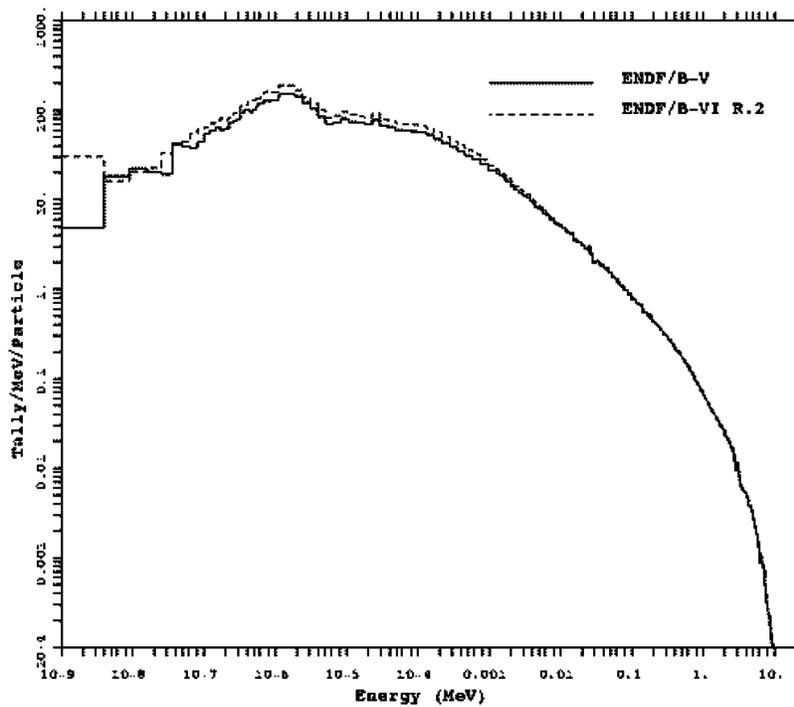**Figure 4: Comparison of Neutron Flux in Central Pu Region of MIXMET8.**

Figure 5: Comparison of Neutron Flux in Graphite Reflector of MIXMET8.
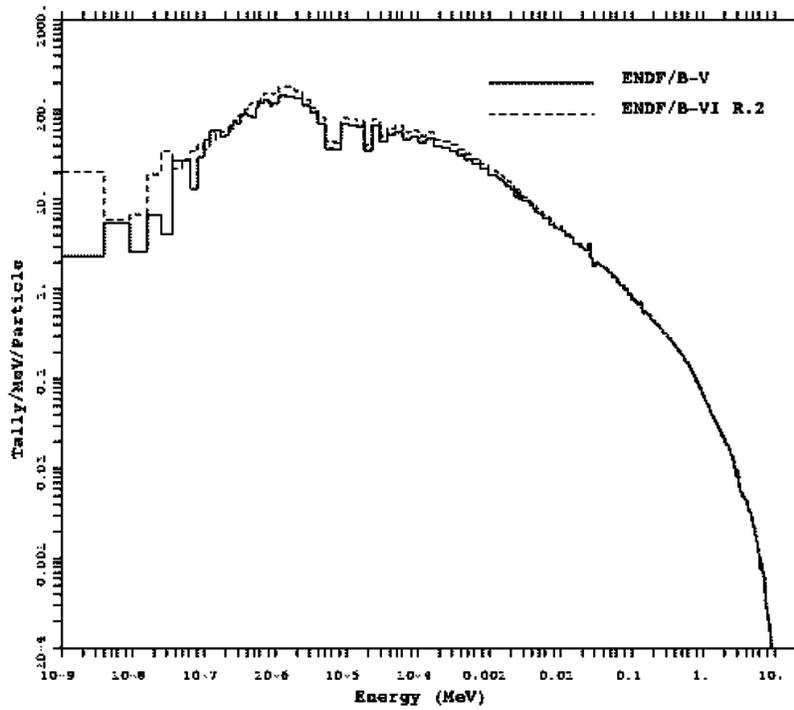
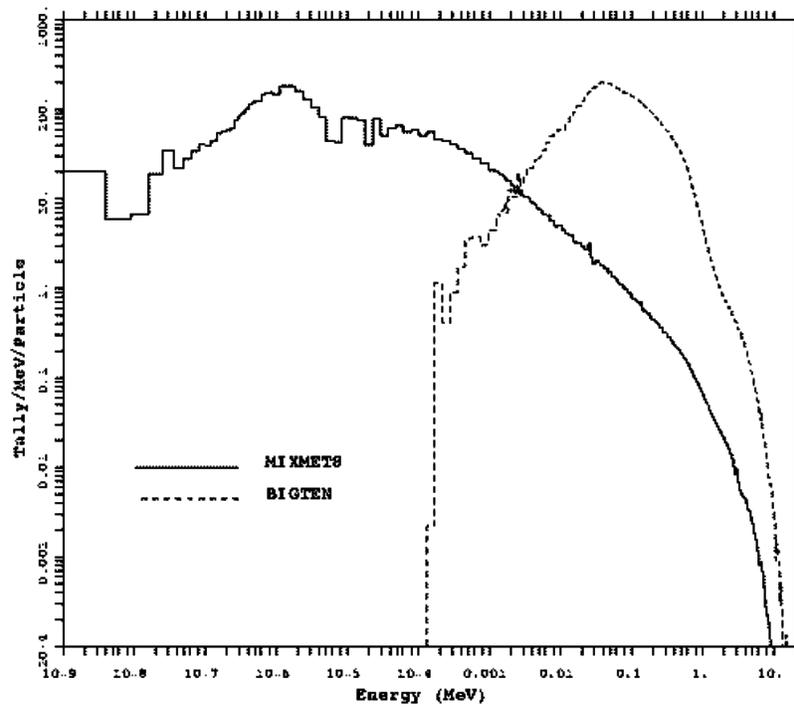**Figure 6: Comparison of Neutron Flux in the Uranium Reflector of MIXMET8.**

Figure 7: Comparison of Neutron Flux in the Uranium Reflector of MIXMET8 and BIGTEN using ENDF/B-VI Data.
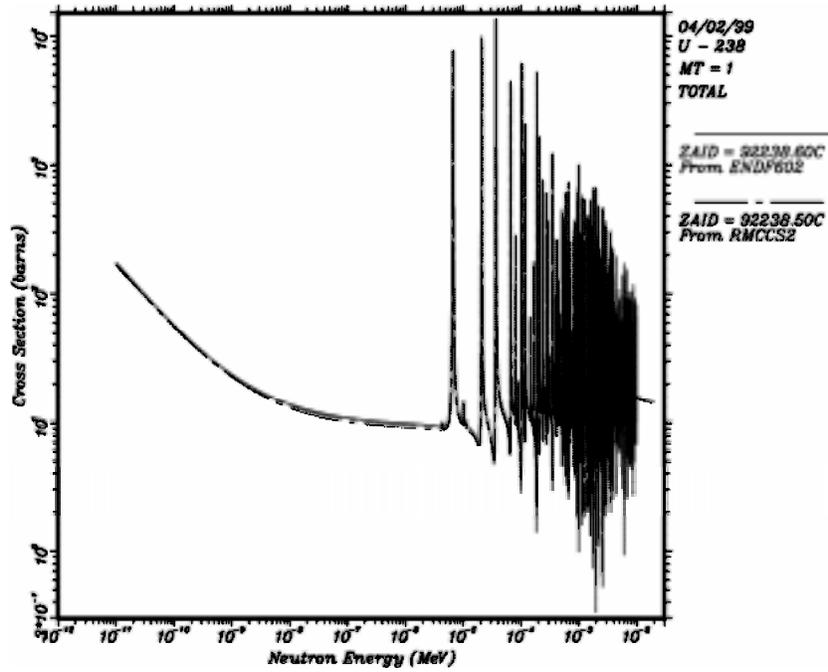
24

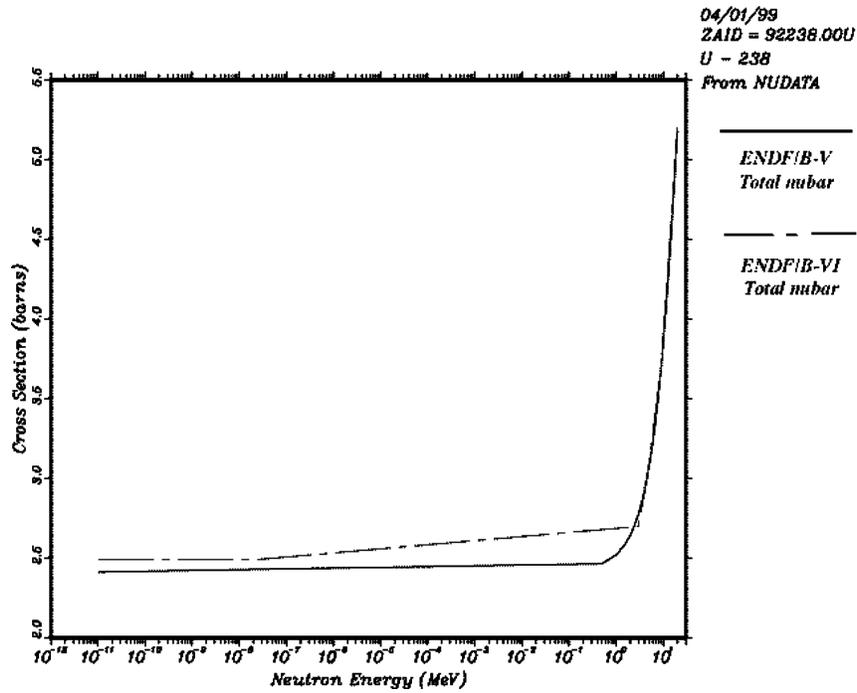**Figure 8: Comparison of the ENDF/B-VI and B-V Total Cross Sections for U-238.**

Figure 9: Comparison of the Total Nubar Data for U-238.

IV.   Summary

A suite of 86 criticality benchmarks for MCNP has been calculated using two sets of continuous-energy neutron data libraries: ENDF/B-VI based data through Release 2 and the ENDF/B-V based data. New evaluations were completed for ENDF/B-VI for a number of the important nuclides such as the isotopes of H, Be, C, N, O, Fe, Ni, ^{235,238}U, ^{237}Np, and ^{239,240}Pu. While this suite of benchmarks covers a wide range of energies and materials, it is no means complete. We anticipate that benchmarks will continue to be added to the suite in the future.

The new evaluations for ^{9}Be, ^{12}C, and ^{14}N showed no net effect on k_{eff}. The results of the solution assemblies indicate that there is a significant decrease in k_{eff} due to the changes in the ^{1}H and ^{16}O evaluations. For the ^{233}U and ^{235}U solution assemblies, this tends to move the k_{eff} value further from the benchmark value, while it tends to move the k_{eff} closer to the benchmark value for ^{239}Pu solutions.

The new evaluations for the Fe and Ni isotopes decreased k_{eff} for the steel- and nickel-reflected assemblies. For Fe, this moved the calculated k_{eff} further from the benchmark value, while the new Ni data moved the calculation closer to the benchmark value. The isotopic tungsten data remained unchanged from B-V to B-VI. The tungsten-reflected assemblies tend to calculate slightly higher than the benchmark values.

Recall that the evaluation for ^{233}U remained unchanged from ENDF/B-V to B-VI, with the exception of the addition of photon production data, which will not affect k_{eff} calculations. For ^{233}U, we find that the one metal assembly, Jezebel-23, calculates slightly low for k_{eff}. The solution assemblies show a drop in k_{eff} when using the ENDF/B-VI based data due to the changes in the ^{1}H and ^{16}O evaluations. For the uranium solutions this tended to move the calculated k_{eff} further from the benchmark value, while it moved the calculated k_{eff} value closer to the benchmark value for plutonium solutions.

For ^{235}U and ^{238}U, we find that for metal (fast) systems, the ENDF/B-VI data for ^{235}U tends to decrease k_{eff} while the ^{238}U data tends to increase k_{eff}. For a given assembly, the energy spectrum and material specifications will determine the net effect for k_{eff}. The HEU metal assemblies tend to show a slight decrease in k_{eff} when using the B-VI data due to ^{235}U. For the more thermal system of the water-reflected HEU

sphere, the ^{235}U data increased k_{eff}. For the ^{235}U solution assemblies, the changes to the ^{235}U evaluation made very little difference.

For the one mixed graphite and U(N)-reflected assembly, a large increase in k_{eff} due to changes in the ^{238}U evaluation moved the calculated k_{eff} much closer to the benchmark value. This result is most probably due to changes below 10 keV where the resonance region was re-evaluated and extended from 4 keV to 10 keV for ENDF/B-VI. The significance of this change indicates the need for more composite benchmarks to exercise as many different energy regions as possible.

There is little change in k_{eff} for the ^{239}Pu metal assemblies. For the solution assemblies, the changes in the ^{239}Pu evaluation tended to decrease k_{eff}, moving the value closer to the benchmark value.

V.   Acknowledgments

VI. References

1   J. F. Briesmeister, Ed., "MCNP4B – A General Monte Carlo N-Particle Transport Code," Los Alamos National Laboratory report LA-12625-M (1997).

2   S. C. Frankle, "A Suite of Criticality Benchmarks for Validating Nuclear Data," Los Alamos National Laboratory report LA-13594 (1999).

3   P. Jaegers and R. Sanchez, "Intermediate Neutron Spectrum Problems and the Intermediate Neutron Spectrum Experiment," Proceedings of the International Topical Meeting on Nuclear and Hazardous Waste Management (American Nuclear Society, La Grange Park, IL, 1996).

4   "Cross Section Evaluation Working Group Benchmark Specifications," ENDF-202, Brookhaven National Laboratory report BNL 19302 (revised 1991).

5   "International Handbook of Evaluated Criticality Safety Benchmark Experiments," NEA Nuclear Science Committee, NEA/NSC/DOC (95)03, 1998 Edition, (http://wastenot.inel.gov/icsbep/handbook.html).

6   J. S. Hendricks, S. C. Frankle, and J. D. Court, "ENDF/B-VI Data for MCNP," Los Alamos National Laboratory report LA-12891 (1994).

7   S. C. Frankle, "Spectral Measurements in Critical Assemblies: MCNP Specifications and Calculated Results," Los Alamos National Laboratory report, to be published in 1999.

8   R. E. MacFarlane and D. W. Muir, "The NJOY Nuclear Data Processing System, Version 91," Los Alamos National Laboratory report LA-12740-M and UC-413 (1994).

9   R. D. Mosteller, S. C. Frankle, and P. G. Young, "Data Testing of ENDF/B-VI with MCNP: Critical Experiments, Thermal-Reactor Lattices, and Time-of-Flight Measurements," *Advances in Nuclear Science and Technology* **24**, 131 (1997).

Los Alamos
NATIONAL LABORATORY

Los Alamos, New Mexico 87545